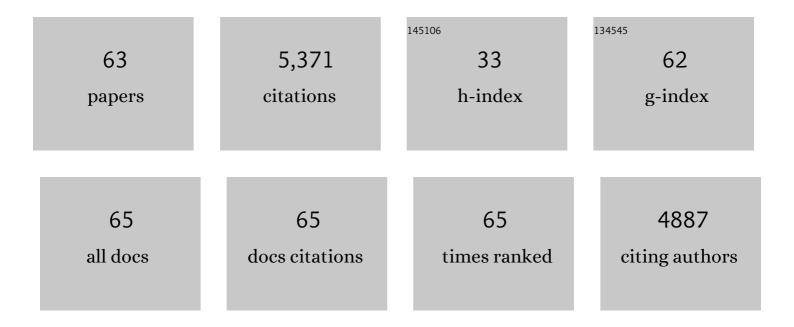
## **Richard A Ferrare**

List of Publications by Year in descending order

Source: https://exaly.com/author-pdf/2876714/publications.pdf Version: 2024-02-01



#	Article	IF	CITATIONS
1	Modeled and observed properties related to the direct aerosol radiative effect of biomass burning aerosol over the southeastern Atlantic. Atmospheric Chemistry and Physics, 2022, 22, 1-46.	1.9	22
2	Polarimeter + Lidar–Derived Aerosol Particle Number Concentration. Frontiers in Remote Sensing, 2022, 3, .	1.3	5
3	Seasonal updraft speeds change cloud droplet number concentrations in low-level clouds over the western North Atlantic. Atmospheric Chemistry and Physics, 2022, 22, 8299-8319.	1.9	9
4	An overview of the ORACLES (ObseRvations of Aerosols above CLouds and their intEractionS) project: aerosol–cloud–radiation interactions in the southeast Atlantic basin. Atmospheric Chemistry and Physics, 2021, 21, 1507-1563.	1.9	97
5	Spatiotemporal Heterogeneity of Aerosol and Cloud Properties Over the Southeast Atlantic: An Observational Analysis. Geophysical Research Letters, 2021, 48, e2020GL091469.	1.5	13
6	Spatiotemporal changes in aerosol properties by hygroscopic growth and impacts on radiative forcing and heating rates during DISCOVER-AQ 2011. Atmospheric Chemistry and Physics, 2021, 21, 12021-12048.	1.9	4
7	Reducing uncertainties in satellite estimates of aerosol–cloud interactions over the subtropical ocean by integrating vertically resolved aerosol observations. Atmospheric Chemistry and Physics, 2020, 20, 7167-7177.	1.9	17
8	Atmospheric Research Over the Western North Atlantic Ocean Region and North American East Coast: A Review of Past Work and Challenges Ahead. Journal of Geophysical Research D: Atmospheres, 2020, 125, e2019JD031626.	1.2	35
9	Aerosol retrievals from different polarimeters during the ACEPOL campaign using a common retrieval algorithm. Atmospheric Measurement Techniques, 2020, 13, 553-573.	1.2	28
10	Ambient Aerosol Hygroscopic Growth From Combined Raman Lidar and HSRL. Journal of Geophysical Research D: Atmospheres, 2020, 125, e2019JD031708.	1.2	13
11	Aerosol Direct Radiative Effect Sensitivity Analysis. Journal of Climate, 2020, 33, 6119-6139.	1.2	32
12	Modeling the smoky troposphere of the southeast Atlantic: a comparison to ORACLES airborne observations from September of 2016. Atmospheric Chemistry and Physics, 2020, 20, 11491-11526.	1.9	32
13	Two decades observing smoke above clouds in the south-eastern Atlantic Ocean: Deep Blue algorithm updates and validation with ORACLES field campaign data. Atmospheric Measurement Techniques, 2019, 12, 3595-3627.	1.2	15
14	Intercomparison of biomass burning aerosol optical properties from in situ and remote-sensing instruments in ORACLES-2016. Atmospheric Chemistry and Physics, 2019, 19, 9181-9208.	1.9	69
15	Novel aerosol extinction coefficients and lidar ratios over the ocean from CALIPSO–CloudSat: evaluation and global statistics. Atmospheric Measurement Techniques, 2019, 12, 2201-2217.	1.2	13
16	Bay Breeze and Sea Breeze Circulation Impacts on the Planetary Boundary Layer and Air Quality From an Observed and Modeled DISCOVERâ€AQ Texas Case Study. Journal of Geophysical Research D: Atmospheres, 2019, 124, 7359-7378.	1.2	35
17	The North Atlantic Aerosol and Marine Ecosystem Study (NAAMES): Science Motive and Mission Overview. Frontiers in Marine Science, 2019, 6, .	1.2	111
18	Aerosol–Cloud–Meteorology Interaction Airborne Field Investigations: Using Lessons Learned from the U.S. West Coast in the Design of ACTIVATE off the U.S. East Coast. Bulletin of the American Meteorological Society, 2019, 100, 1511-1528.	1.7	51

**RICHARD A FERRARE** 

#	Article	IF	CITATIONS
19	Intercomparison of airborne multi-angle polarimeter observations from the Polarimeter Definition Experiment. Applied Optics, 2019, 58, 650.	0.9	28
20	Biomass Burning Plumes in the Vicinity of the California Coast: Airborne Characterization of Physicochemical Properties, Heating Rates, and Spatiotemporal Features. Journal of Geophysical Research D: Atmospheres, 2018, 123, 13,560.	1.2	25
21	Analysis of the Planetary Boundary Layer Height during DISCOVER-AQ Baltimore–Washington, D.C., with Lidar and High-Resolution WRF Modeling. Journal of Applied Meteorology and Climatology, 2018, 57, 2679-2696.	0.6	15
22	Coupled Retrieval of Liquid Water Cloud and Aboveâ€Cloud Aerosol Properties Using the Airborne Multiangle SpectroPolarimetric Imager (AirMSPI). Journal of Geophysical Research D: Atmospheres, 2018, 123, 3175-3204.	1.2	28
23	Retrieval of Cloud Condensation Nuclei Number Concentration Profiles From Lidar Extinction and Backscatter Data. Journal of Geophysical Research D: Atmospheres, 2018, 123, 6082-6098.	1.2	16
24	Simultaneous polarimeter retrievals of microphysical aerosol and ocean color parameters from the "MAPP―algorithm with comparison to high-spectral-resolution lidar aerosol and ocean products. Applied Optics, 2018, 57, 2394.	0.9	73
25	On the Limits of CALIOP for Constraining Modeled Free Tropospheric Aerosol. Geophysical Research Letters, 2018, 45, 9260-9266.	1.5	22
26	Calibration of a high spectral resolution lidar using a Michelson interferometer, with data examples from ORACLES. Applied Optics, 2018, 57, 6061.	0.9	51
27	The MERRA-2 Aerosol Reanalysis, 1980 Onward. Part I: System Description and Data Assimilation Evaluation. Journal of Climate, 2017, 30, 6823-6850.	1.2	739
28	Saharan dust, convective lofting, aerosol enhancement zones, and potential impacts on ice nucleation in the tropical upper troposphere. Journal of Geophysical Research D: Atmospheres, 2017, 122, 8833-8851.	1.2	16
29	The impact of lidar detection sensitivity on assessing aerosol direct radiative effects. Geophysical Research Letters, 2017, 44, 9059-9067.	1.5	24
30	HSRL-2 aerosol optical measurements and microphysical retrievals vs. airborne in situ measurements during DISCOVER-AQ 2013: an intercomparison study. Atmospheric Chemistry and Physics, 2017, 17, 7229-7243.	1.9	46
31	Aerosol and cloud microphysics covariability in the northeast Pacific boundary layer estimated with shipâ€based and satellite remote sensing observations. Journal of Geophysical Research D: Atmospheres, 2017, 122, 2403-2418.	1.2	15
32	Information content and sensitivity of the 3 <i>β</i> +′ <i>α</i> lidar measurement sy aerosol microphysical retrievals. Atmospheric Measurement Techniques, 2016, 9, 5555-5574.	st <b>er2</b> for	54
33	Combined Atmospheric and Ocean Profiling from an Airborne High Spectral Resolution Lidar. EPJ Web of Conferences, 2016, 119, 22001.	0.1	21
34	The Two olumn Aerosol Project: Phase l—Overview and impact of elevated aerosol layers on aerosol optical depth. Journal of Geophysical Research D: Atmospheres, 2016, 121, 336-361.	1.2	33
35	Retrieval of aerosol parameters from multiwavelength lidar: investigation of the underlying inverse mathematical problem. Applied Optics, 2016, 55, 2188.	2.1	36
36	Regional characteristics of the relationship between columnar AOD and surface PM 2.5 : Application of lidar aerosol extinction profiles over Baltimore–Washington Corridor during DISCOVER-AQ. Atmospheric Environment, 2015, 101, 338-349.	1.9	38

**RICHARD A FERRARE** 

#	Article	IF	CITATIONS
37	Vertically resolved separation of dust and other aerosol types by a new lidar depolarization method. Optics Express, 2015, 23, 14095.	1.7	13
38	Looking through the haze: evaluating the CALIPSO level 2 aerosol optical depth using airborne high spectral resolution lidar data. Atmospheric Measurement Techniques, 2014, 7, 4317-4340.	1.2	69
39	Airborne Multiwavelength High Spectral Resolution Lidar (HSRL-2) observations during TCAP 2012: vertical profiles of optical and microphysical properties of a smoke/urban haze plume over the northeastern coast of the US. Atmospheric Measurement Techniques, 2014, 7, 3487-3496.	1.2	79
40	Separating mixtures of aerosol types in airborne High Spectral Resolution Lidar data. Atmospheric Measurement Techniques, 2014, 7, 419-436.	1.2	79
41	An evaluation of CALIOP/CALIPSO's aerosolâ€aboveâ€cloud detection and retrieval capability over North America. Journal of Geophysical Research D: Atmospheres, 2014, 119, 230-244.	1.2	49
42	Arrange and average algorithm for the retrieval of aerosol parameters from multiwavelength high-spectral-resolution lidar/Raman lidar data. Applied Optics, 2014, 53, 7252.	2.1	27
43	Observations of rapid aerosol optical depth enhancements in the vicinity of polluted cumulus clouds. Atmospheric Chemistry and Physics, 2014, 14, 11633-11656.	1.9	58
44	Comparison of mixed layer heights from airborne high spectral resolution lidar, ground-based measurements, and the WRF-Chem model during CalNex and CARES. Atmospheric Chemistry and Physics, 2014, 14, 5547-5560.	1.9	70
45	Evaluation of surface and upper air fine scale WRF meteorological modeling of the May and June 2010 CalNex period in California. Atmospheric Environment, 2013, 80, 299-309.	1.9	41
46	Aerosol classification using airborne High Spectral Resolution Lidar measurements – methodology and examples. Atmospheric Measurement Techniques, 2012, 5, 73-98.	1.2	407
47	Assessment of the CALIPSO Lidar 532 nm attenuated backscatter calibration using the NASA LaRC airborne High Spectral Resolution Lidar. Atmospheric Chemistry and Physics, 2011, 11, 1295-1311.	1.9	111
48	An accuracy assessment of the CALIOP/CALIPSO version 2/version 3 daytime aerosol extinction product based on a detailed multi-sensor, multi-platform case study. Atmospheric Chemistry and Physics, 2011, 11, 3981-4000.	1.9	94
49	Observations of Saharan dust microphysical and optical properties from the Eastern Atlantic during NAMMA airborne field campaign. Atmospheric Chemistry and Physics, 2011, 11, 723-740.	1.9	80
50	LASE Measurements of Water Vapor, Aerosol, and Cloud Distributions in Saharan Air Layers and Tropical Disturbances. Journals of the Atmospheric Sciences, 2010, 67, 1026-1047.	0.6	34
51	The CALIPSO Automated Aerosol Classification and Lidar Ratio Selection Algorithm. Journal of Atmospheric and Oceanic Technology, 2009, 26, 1994-2014.	0.5	820
52	The Saharan Air Layer and the Fate of African Easterly Waves—NASA's AMMA Field Study of Tropical Cyclogenesis. Bulletin of the American Meteorological Society, 2009, 90, 1137-1156.	1.7	119
53	NASA LaRC airborne high spectral resolution lidar aerosol measurements during MILAGRO: observations and validation. Atmospheric Chemistry and Physics, 2009, 9, 4811-4826.	1.9	100
54	Aerosol and cloud interaction observed from high spectral resolution lidar data. Journal of Geophysical Research, 2008, 113, .	3.3	76

**RICHARD A FERRARE** 

#	Article	IF	CITATIONS
55	Airborne High Spectral Resolution Lidar for profiling aerosol optical properties. Applied Optics, 2008, 47, 6734.	2.1	430
56	Application of aerosol hygroscopicity measured at the Atmospheric Radiation Measurement Program's Southern Great Plains site to examine composition and evolution. Journal of Geophysical Research, 2006, 111, .	3.3	26
57	Comparison between lidar and nephelometer measurements of aerosol hygroscopicity at the Southern Great Plains Atmospheric Radiation Measurement site. Journal of Geophysical Research, 2006, 111, .	3.3	45
58	Use of in situ cloud condensation nuclei, extinction, and aerosol size distribution measurements to test a method for retrieving cloud condensation nuclei profiles from surface measurements. Journal of Geophysical Research, 2006, 111, .	3.3	39
59	Evaluation of daytime measurements of aerosols and water vapor made by an operational Raman lidar over the Southern Great Plains. Journal of Geophysical Research, 2006, 111, .	3.3	71
60	Automated Retrievals of Water Vapor and Aerosol Profiles from an Operational Raman Lidar. Journal of Atmospheric and Oceanic Technology, 2002, 19, 37-50.	0.5	110
61	Raman lidar profiling of water vapor and aerosols over the Southern Great Plains. , 2001, , .		6
62	Raman lidar measurements of aerosol extinction and backscattering: 2. Derivation of aerosol real refractive index, single-scattering albedo, and humidification factor using Raman lidar and aircraft size distribution measurements. Journal of Geophysical Research, 1998, 103, 19673-19689.	3.3	74
63	Raman lidar system for the measurement of water vapor and aerosols in the Earth's atmosphere. Applied Optics, 1992, 31, 3068.	2.1	363